Fermi National Accelerator Laboratory

FERMILAB-Conf-91/223-E

Results from $\bar{p}p$ Colliders

J. Huth
Fermi National Accelerator Laboratory
P.O. Box 500, Batavia, Illinois 60510

August 1991

* Presented at *Particles and Fields '91*, University of Vancouver, Vancouver, B. C., Canada, August 18-22, 1991

CDF/PUB/CDF/PUBLIC/1555
FERMILAB CONF-91/223-E

RESULTS FROM $\bar{p}p$ COLLIDERS

JOHN HUTH
Mail Station 318, Fermilab
Batavia, IL 60510 USA

ABSTRACT

Recent results from $\bar{p}p$ colliders are presented. From elastic scattering experiments at the Tevatron, an average value of $\sigma_{tot} = 72.1 \pm 2$ mb is reported, along with a new measurement of $\rho = 0.13 \pm 0.7$. New measurements of jet, direct photon and high p_t W and Z production are compared to more precise, higher order predictions from perturbative QCD. Recently available data on the W mass and width give combined values for $M_W = 80.14 \pm 0.27$ GeV/c^2, and $\Gamma(W) = 2.14 \pm 0.08$ GeV. From electroweak radiative corrections and M_W, one finds $M_{top} = 130 \pm 40$ GeV/c^2, with a 95 % C.L. upper limit at 210 GeV/c^2. Current limits on M_{top} are presented, along with a review of the prospects for top discovery. From jet data there is no evidence of quark substructure down to the distance scale of 1.4×10^{-17} cm, nor is there evidence for supersymmetry or heavy gauge bosons at $\bar{p}p$ colliders, allowing lower limits on $M_{W'} > 520$ GeV/c^2 and $M_{Z'} > 412$ GeV/c^2.

1. *Log s* Physics

The total cross section, $\sigma_{tot}(\bar{p}p)$, can be determined using the optical theorem, and extrapolating the elastic cross section to $t = 0$:

$$\sigma_{tot}^2 = 16\pi(\hbar c)^2(1+\rho^2)^{-1}\frac{d\sigma^{el}}{dt}|_{t=0} \qquad (1)$$

where ρ is the ratio of the real to imaginary cross section at $t = 0$. Below S$\bar{p}p$S energies, one finds typical ρ values less than 0.1, but an anomalously high measurement of $\rho = 0.24 \pm 0.04$ has been reported by the UA4 collaboration[1] at the S$\bar{p}p$S Collider (CMS energy of 630 GeV). Both the CDF[3] and E710[4] collaborations have reported recent measurements of σ_{tot} at the Tevatron Collider (1800 GeV), and E710 has reported a measurement of ρ.

Both groups use the above expression, but employ different techniques to derive σ_{tot}. E710 relies on a luminosity independent method. One can also write σ_{tot} as the sum of the inelastic and elastic rates:

$$\sigma_{tot} = (N_{el} + N_{inel})/\mathcal{L} \qquad (2)$$

Published Proceedings Particles and Fields '91, University of Vancouver, Vancouver, British Columbia, Canada, August 18-22, 1991.

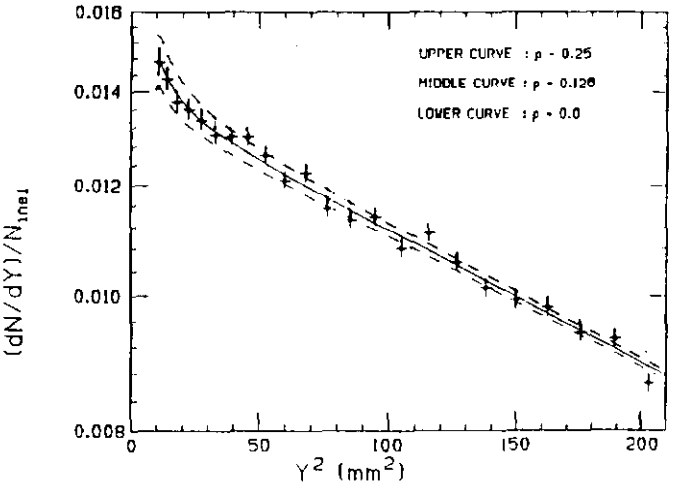

Figure 1: Elastic scattering rate from the E710 experiment, plotted as a function of Y, the distance from the beam in one of the detectors. The region of Coulomb and nuclear interfence is apparent at small Y values.

where $\mathcal{L}$ is the integrated luminosity. Substituting this into the previous equation, one can find a luminosity independent expression for σ_{tot}:

$$\sigma_{tot} = \frac{16\pi(\hbar c)^2 \frac{dN_{el}}{dt}|_{t=0}}{(1+\rho^2)(N_{el}+N_{inel})} \tag{3}$$

E710 measures the elastic rate using a set of low angle chambers in the beamline, and the inelastic rate measured using a set of scintillators surrounding the interaction region. Figure 1 shows the elastic rate as a function of distance from the beam from E 710. The point on the far left corrseponds to $t = 0.001$ GeV/c^2, where the interference between the Coulomb and nuclear terms is apparent. ρ can be extracted from the interference region using the calculated Coulomb phase. E710's ρ value, 0.13 ± 0.07, is consistent with values found at energies below S$\bar{p}p$S Collider energies, but not of sufficient precision make a definitive statement about the UA4 result. From ρ, the elastic slope, and the inelastic rate, they obtain $\sigma_{tot} = 72.8 \pm 3.0$ mb.[4]

In contrast to E710, CDF[3] uses a direct measurement of the accelerator parameters to calculate the luminosity, and hence make a direct extrapolation to $t = 0$. The CDF detector also consists of a series of chambers which can be inserted into the beamline. The determination of the luminosity is reasonably precise ($\pm$ 8 %), and a value of σ_{tot} =71.5 $\pm$ 3.0 mb is found, assuming $\rho = 0.145$. A wide range of ρ, is included in the systematic uncertainty. Figure 2 shows σ_{tot} as a function of $\sqrt{s}$ and with extrapolations from lower energies by Block and Cahn. The results from both E710 and CDF are in agreement and show a preference for an asymptotically flat extrapolation over an asymptotic form of $log^2(s/s_o)$.[5] The E710 and CDF results can be averaged to obtain σ_{tot} =72.1$\pm$2 mb.

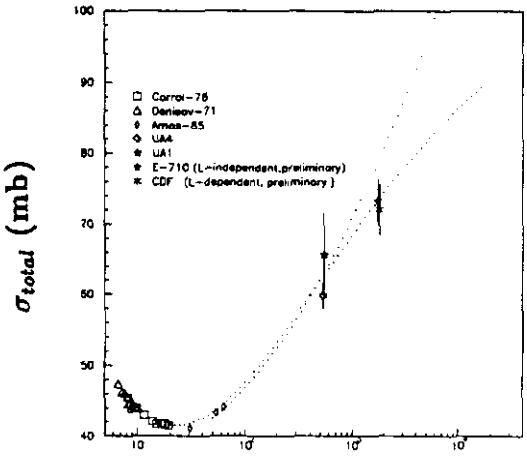

Figure 2: Total cross section in $\bar{p}p$ collisions as a function of CMS energy. The recent results from both the CDF and E710 collaborations are indicated at 1.8 TeV. The dotted lines represent possible extrapolations from lower energies predicted by Block and Cahn.[5] The upper curve corresponds to an extrapolation with an asymptotic form $ln^2 s/s_o$, the lower curve has a flat asymptote.

2. Tests of QCD

2.1. Inclusive Jet Production

Jet production probes the highest values of Q^2 typically available at accelerator energies. In the past, the precision of the comparison of data to theory has been hampered by both large experimental and theoretical uncertainties. With the advent of new $\mathcal{O}(\alpha_s^3)$ predictions of the cross section,[9–11] the theoretical precision has improved substantially (10 % vs. 50 %). Infinities can arise in the calculations if partons are allowed to become conllinear or very soft; some kind of procedure must be imposed to define a "jet" rather than a parton cross section to obtain finite results. The experimentalist uses a grid of calorimeter towers which are typically segmented in equal units of azimuth ϕ and pseudorapidity $\eta \equiv -ln\, tan\theta/2$ (θ is the polar angle) to measure energy flow, and defines a jet in terms of clusters of energy. To take advantage of the improvements in theory, there must be a common definition of a "jet" at both the experimental and theoretical level. A recent proposal, the "Snowmass Accord",[12] attempts to standardize the definition of a jet. The agreement adopts a *cone* algorithm with a radius of $R \equiv \sqrt{\Delta\phi^2 + \Delta\eta^2} = 0.7$ defined, where clusters of energy or partons occuring inside this cone are merged to form a jet.

Experimental systematic uncertainties, dominated by the knowledge of jet energy scale, have been shrinking. In the past, the uncertainties on the cross section was of order $\geq$ 50 %,[13–15] whereas now both CDF and UA2[16] report $\approx$ 20-30 % uncertainties. Figure 4 shows recent measurements of inclusive jet cross section, $\sigma(\bar{p}p \rightarrow JET + X)$,

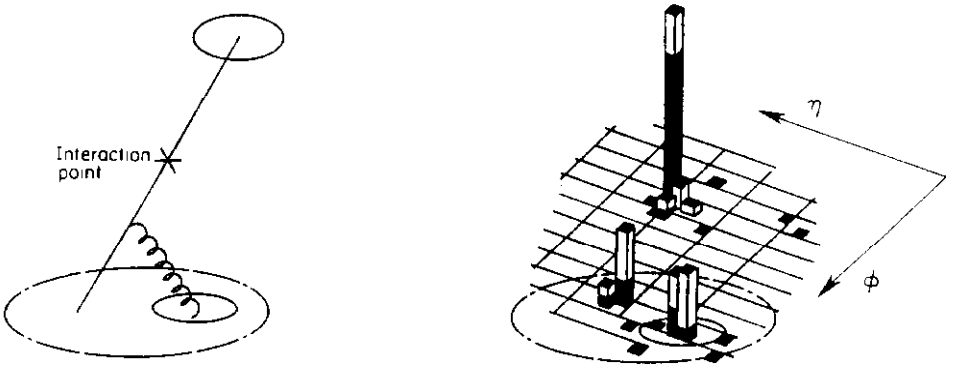

Figure 3: Jet definition as viewed by a theorist and by an experimentalist. A consistent definition of a "jet" must be adopted to take advantage of the improved precision offered by higher order calculations (figure 3). The size of the clustering cone, and the prescription for merging partons/energy must be the same.

plotted as a function of jet E_t for both experiments. Only one set of parton distribution functions (HMRSB[7]) was used, and the absolute normalizations of QCD and the experiments were used to produce this figure. The most impressive feature is the agreement of the QCD calculation[11] over so many orders of magnitude in cross section. On a linear scale, a plot of (data-theory)/theory (figure 4) from CDF data shows compares several parton distribution functions (PDF). The HMRSB[7] and MT[8] PDF's give acceptable fits to the data, but the HMRSE set gives a poor fit to the CDF jet data. A unique feature the $\mathcal{O}(\alpha_s^3)$ prediction is the variation of the jet cross section with cone size R. This is shown in figure 5 for 100 GeV E_t jets from CDF data. The three curves represent a range of theory predictions. For these conditions, a cone size of $R \approx 0.7$ appears to minimize theoretical uncertainties.

At high energy, the shape of jets is greatly determined by hard gluon radiation, not by hadronization, as is true for lower energy jets (discussed by N. Wainer at this conference). To measure shape, one can compare the fraction of E_t inside a inner cone, of radius r to the total jet E_t. CDF has measured this using tracking data for jets clustered with a cone of $R = 1.0$. Figure 6, shows this distribution for 100 GeV jets derived from CDF data. Also shown are the $\mathcal{O}(\alpha_s^3)$ predictions for jet shapes,[17] along with the predictions of the event generator HERWIG.[18]

2.2. Multi-Jet Production

To date, multijet cross sections and topologies have been predicted by QCD only at tree level (*i.e.* graphs which do not include virtual corrections). Tree level calculations are also commonly used for predicting the production and topology of W plus jet events, which form an important background for top searches. One of the better testing grounds for these predictions is in multijet events. A comparison of three jet toplogies with these calculations has been performed by CDF. Of the six independent

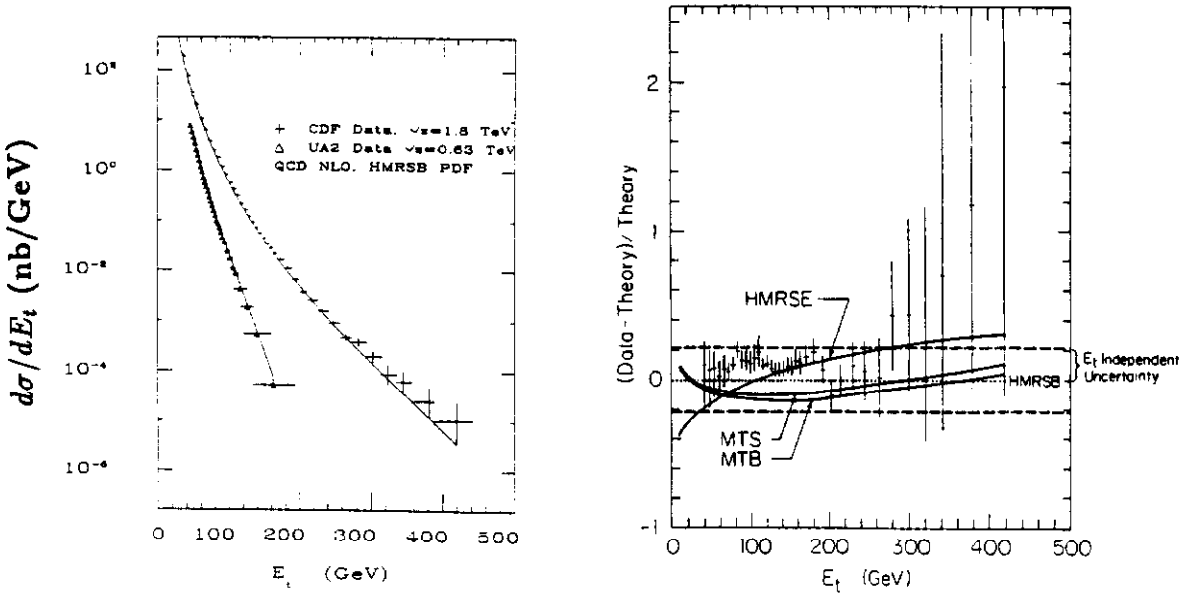

Figure 4: Inclusive jet cross sections from the CDF and UA2 experiments compared to the predictions of an $\mathcal{O}(\alpha_s^3)$ QCD prediction.[10,11] All normalizations are absolute. Also shown is the ratio of (data-theory)/theory plotted for different choices of parton distribution functions.

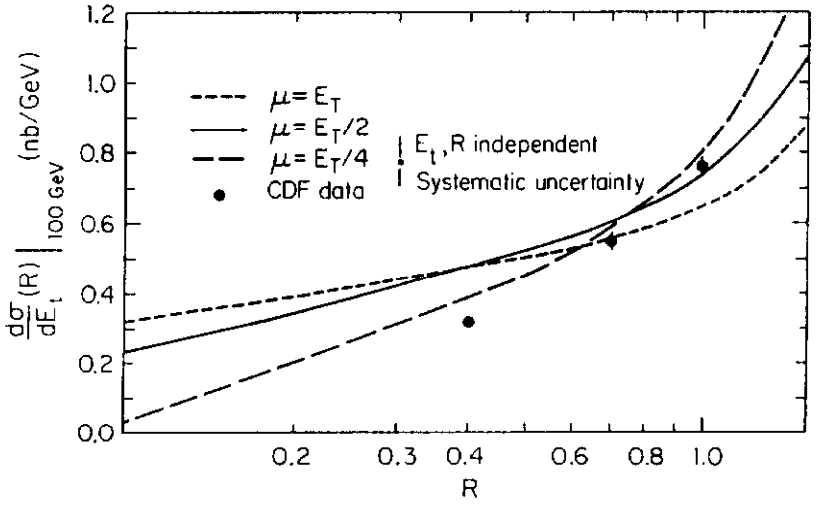

Figure 5: Variation of the CDF jet cross section for $E_t = 100$ GeV with clustering cone radius, R. The curves represent a range of theoretical predictions from an $\mathcal{O}(\alpha_s^3)$ calculation.

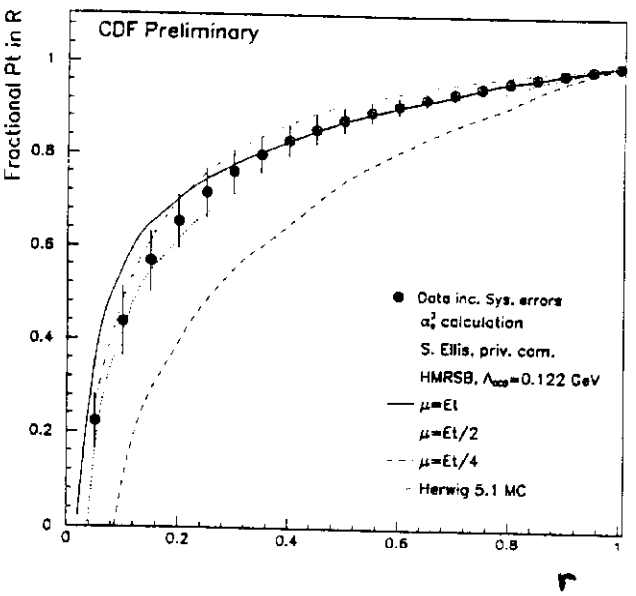

Figure 6: Jet shape, defined in text for 100 GeV E_t jets from CDF. The curves are from an $\mathcal{O}(\alpha_s^3)$ parton level calculation, and also from the HERWIG event generator.[18]

variables that describe the three jet system in the event center-of-mass frame, CDF have focused on four: a) the energy fraction carried by the leading jet $x_3 = 2E_3/M_{3j}$ and b) by the next-to-leading jet $x_4 = 2E_4/M_{3j}$, c) the polar angle of the lead jet, θ^*, and d) ψ^*, the angle between the plane containing the beam and the lead jet and the 3 jet event plane.

CDF defines an event sample with at least three jets, each with $E_t \geq 15$ GeV, from data selected with a total transverse energy trigger (> 120 GeV). A minimum three jet invariant mass is required, $M_{3j} > 250$ GeV/c^2, and the acceptance is flat to within $\approx 7\%$ for each variable. Tree level matrix elements[20,21] form inputs to a detector simulation, where Monte Carlo events are subjected to the same cuts as the data. Figure 7 shows the comparison of data and theory for the x_3 and ψ^* distributions. Pure two-jet events would produce a spike at x_3 =1.0. The solid line indicates the QCD prediction. The dashed line indicates the prediction if only $\bar{q}q$ initial states contributed. The other two variables, x_4 and $cos\theta^*$ also are also sensitive to whether the initial state is glue-glue, quark-glue or quark-antiquark. A global fit to all four distributions was made where the $\bar{q}q$ fraction in the initial state is fitted as a free parameter. The resulting fraction is 3^{+7}_{-3} %, consistent with the tree level prediction of 11$\pm$4 %. The three jet cross section, given the event selection is 1.2 $\pm$ 0.02 (stat) $\pm$ 0.6 (syst) nb, whereas the tree level prediction is 1.8$\pm$0.9 nb. Although the cross sections are consistent, the uncertainties are considerable. The main experimental uncertainty is from the energy scale for jets. The dominant theoretical uncertainty is related to the momentum scale used to evaluate the strong coupling constant, α_s and the parton distribution functions;

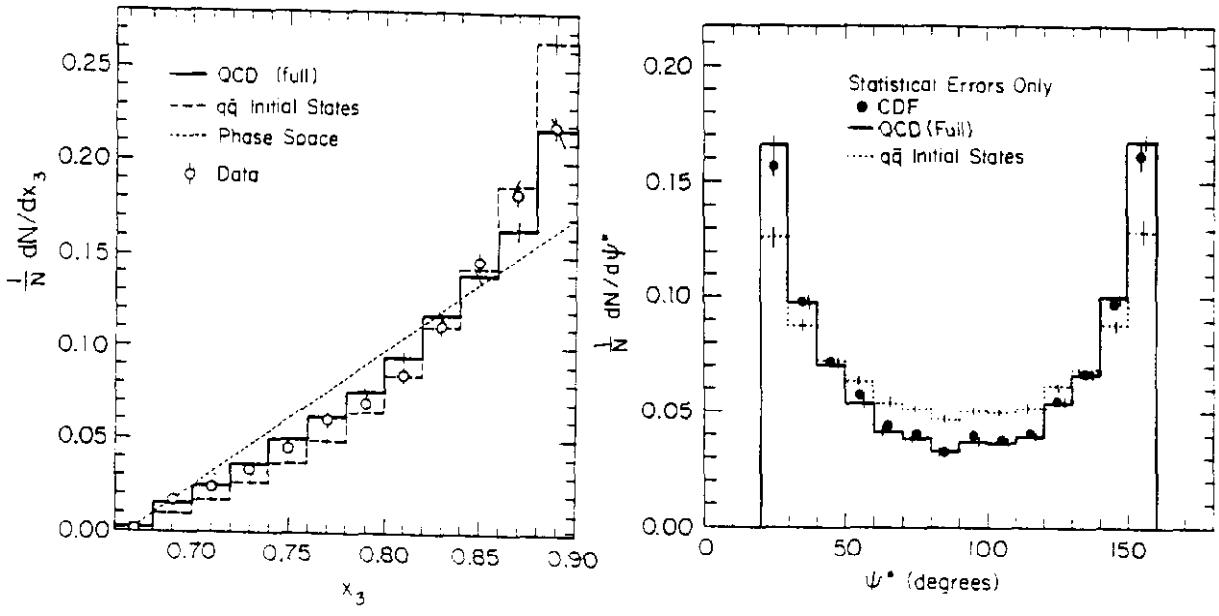

Figure 7: Variables for three jet events, x_3 and ψ^*, showing the data, the predictions of QCD, and the prediction from $\bar{q}q$ initial states only. The data are compatible with the small expected fraction of $\bar{q}q$ in the initial states.

this large uncertainty is typical of tree level predictions.

UA2 has made a comparison of five and six jet cross sections to tree level predictions. They define a sample of jets with $E_{ti} > 15$ GeV, and $|\eta_i| < 2.0$. With this selection, they observe 281 five-jet events and 7 six-jet events, and derive cross sections of 1.31 and 0.037 nb respectively. The cross sections have uncertainties of $\pm$ 60 %, also from energy scale uncertainties. QCD predicts cross sections with large uncertainties (factor of 2) of 1.28 nb for five-jet events and 0.040 nb for six-jet events.

2.3. High P_t W and Z Production

W and Z production is described in leading order in perturbation theory by the Drell-Yan mechanism. At higher orders, the W and Z can recoil against a quark or gluon to obtain a finite kick in the transverse plane (figure 8). For small W or Z p_t's, one must rely on a summation of leading terms from soft gluons to all orders to obtain the cross section. This is particularly important in obtaining the W mass. When the W p_t is high enough to be associated with jet production, the leading terms in perturbation theory should give a reasonable description of the data. CDF has measured the inclusive W and Z p_t distribution at $\sqrt{s} = 1.8$ TeV. The W p_t distribution has to correct for the missing E_t carried away from the neutrino, and an unfolding procedure must be applied to take into account the finite jet energy resolution. The Z p_t distribution can, in principle, be measured more accurately, because the dilepton final state can be measured precisely, but suffers from lower statistics. The results are shown in figure 9. The QCD predictions at next-to-leading order,[23] $\mathcal{O}(\alpha_s^2, \alpha_{em})$, provide a good description

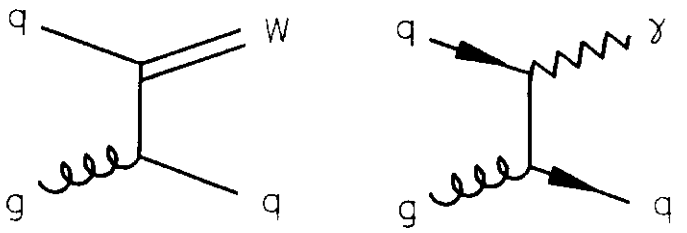

Figure 8: Similar graphs appearing at $\mathcal{O}(\alpha_{em}, \alpha_s)$ for photon and high p_t W.

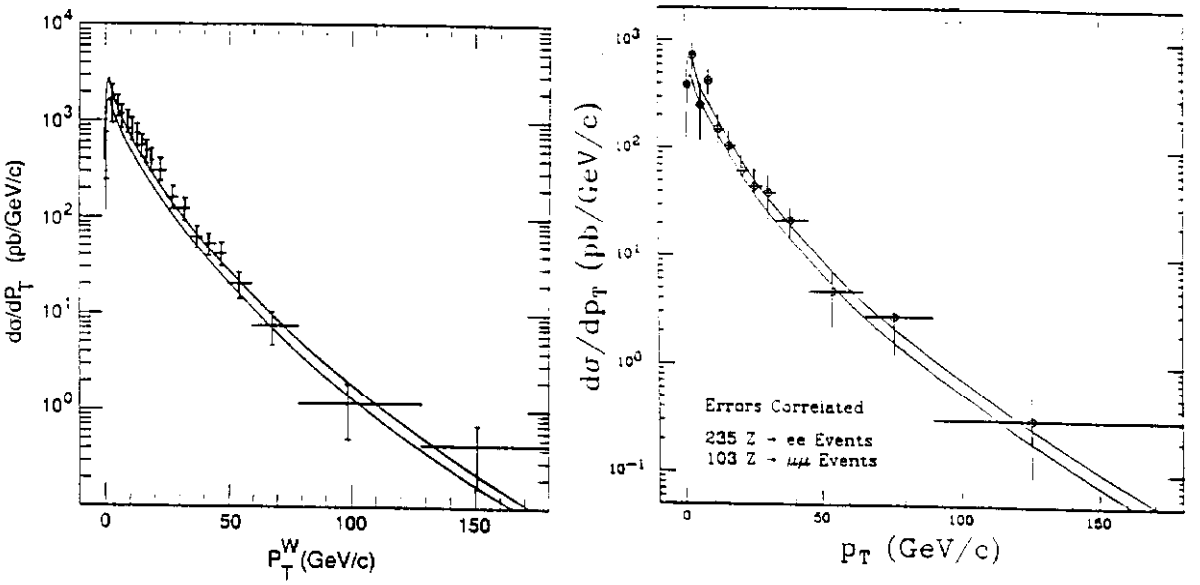

Figure 9: p_t distributions for W and Z bosons in the CDF experiment. The curves are from the theoretical predictions of Arnold, Kauffman and Reno.[23]

of the data, and there is no significant excess apparent at high p_t.

The UA2 collaboration has used the ratio of $W + 1$ jet to $W + 0$ jet events to obtain a measure of α_s evaluated at the W mass. Here, the jet is required to have an E_t greater than 20 GeV. With 2845 $W + 0$ jet and 114 $W + 1$ jet events, the ratio is 3.9±0.4 %. A tree level Monte Carlo program is used to generate events as input to a detector simulation. After taking into account the effect of virtual corrections, a value of $\alpha_s(M_W)$ =0.123 ± 0.018 (stat) ± 0.017 (syst), is obtained. The systematic uncertainty has contributions from the choice of fragmentation model, the underlying event modeling and jet energy scale.[26] This is consistent with the recent value reported from LEP ($\alpha_s(M_Z)$ =0.118±0.008).[22]

2.4. Direct Photon Production

In principle, the direct photon production cross section, $\sigma(\overline{p}p \rightarrow \gamma + X)$, provides one of the best probes of the low x region of the gluon structure functions. Theoretical progress has been made in producing next-to-leading order QCD predictions ($\mathcal{O}(\alpha_s^2, \alpha_{em})$).[27-29] Both UA2 and CDF must initially impose some kind of isolation

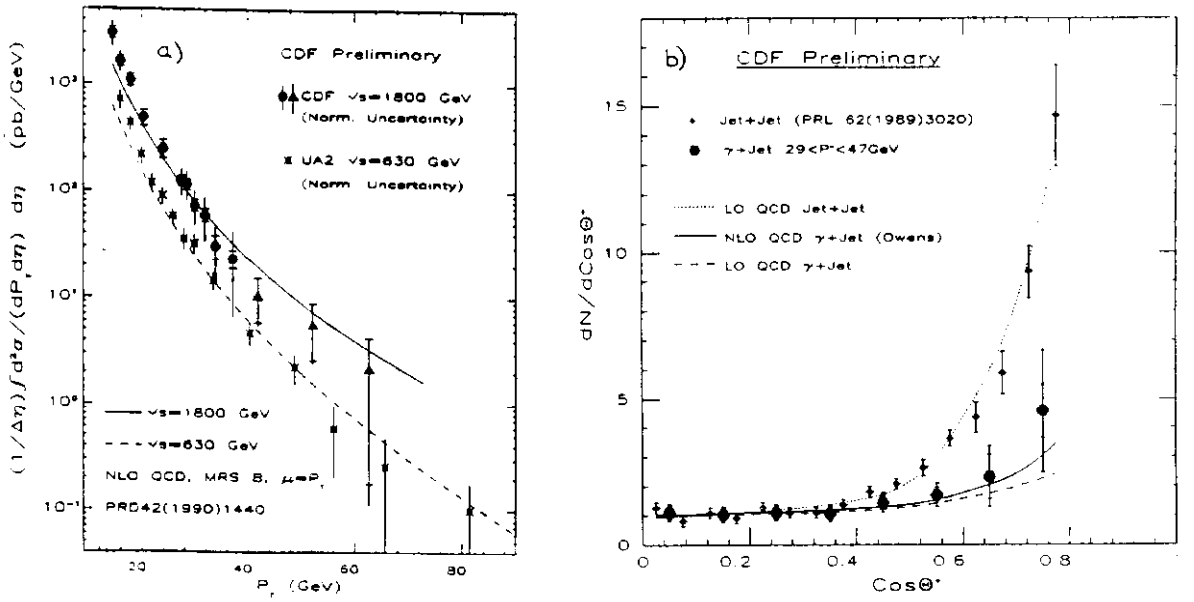

Figure 10: Direct photon cross section measured by the UA2 ($\sqrt{s}$ =0.63 TeV) and the CDF ($\sqrt{s}$ =1.8 TeV) experiments. The lines are the predictions of a next-to-leading order QCD prediction.[27] On the right is the γ−jet angular distribution in the CMS frame ($cos\theta^*$). Also shown is the jet-jet angular distribution, measured in a similar kinematic range. The QCD predictions for both processes are indicated.

cone around the photon in order to reduce the serious background of π^o's in jets. CDF uses a cone of 0.7 units in the $\eta - \phi$ metric, whereas UA2 uses a cone of 0.265 units.

UA2 relies on a photon converter to distinguish isolated photons from π^o decays. Conversions are identified in a scintillating fiber array beyond a lead converter (1.5 X_o). The conversion probability for photons is roughly constant as a function of photon energy, and hence a statistical subtraction of the π^o contribution is possible up to relatively high photon E_t. CDF also uses a conversion technique, employing the outer wall of their central tracking chamber as a photon converter ($\approx 0.2X_o$), followed by a series of drift tubes which provide information on the conversions. These conversion data are limited by statistics due to the small wall thickness. CDF relies primarily on measurements of the shape of the transverse EM shower profile near shower maximum to statistically separate narrow photon showers from the broader π^0 induced showers. The results from both experiments are displayed in figure 10, along with the predictions of a next-to-leading order QCD prediction by Aurenche *et al.*[27] Both sets of data appear to be running higher than the indicated theory at low E_t. The calculations are not evaluated fully at $\mathcal{O}(\alpha_s^2, \alpha_{em})$ as the contribution from bremsstrahlung off of quark lines is only approximated. It is possible that a full calculation may improve the comparison between theory and experiment.

The γ−jet CMS angular distribution is sensitive to the dynamics of direct photon

production, which proceeds at leading order with graphs involving the exchange of quarks (figure 8). As reported by R. Harris at this meeting, CDF has measured the angular distribution as a function of $cos\theta^*$ for photon-jet events. This is shown in figure 10, along with the distribution from jet-jet events in a similar kinematic range. Because the $\gamma-$jet events come predominantly from spin-$\frac{1}{2}$ quark exchange, the angular distribution is not the same as for jet-jet scattering, which is dominated by spin-1 gluon exchange at small angles.

3. Electroweak Measurements

3.1. M_W

Measurements of the intermediate vector bosons have gone well beyond the discovery stage and into a regime where improved precision and calculations of radiative corrections define a window on the top, and possibly the Higgs. The relation between the electroweak parameters can be expressed using the convention of Marciano and Sirlin[30]:

$$sin^2\theta_W = \frac{A^2}{M_W^2(1-\Delta r)} \tag{4}$$

where $A = (\pi\alpha/\sqrt{2}G_\mu)^{1/2} = 37.2805 \pm 0.0003$ GeV, $sin^2\theta_W = 1 - M_W^2/M_Z^2$ and Δr is a radiative correction involving, among other parameters, the unknown M_{top} and M_{Higgs}. From these constraints, a precise determination of M_W, in combination with M_Z from e^+e^- colliders, can constrain M_{top}, and even partially M_{Higgs}. If top is (or isn't) found then constraints on the standard model can be checked.

The most recent measurements of M_W and $\Gamma(W)$ have been reported by CDF[31] and UA2.[32] Both UA2 and CDF use the $W \rightarrow e\nu$ decay mode. CDF also has a measurement in the $W \rightarrow \mu\nu$ channel. Because the neutrino is undetected, its momentum must be inferred. Furthermore, because all events have a longitudinal boost, one can only impose momentum conservation in the transverse plane. The transverse momentum, $p_{t\nu}$ of the neutrino is calculated from the vector sum of the momenta of all the visible transverse energy. Figure 11 shows the transverse mass, $M_t \equiv \sqrt{2p_{te}p_{t\nu}(1-cos(\phi_{e\nu}))}$ for $e\nu$ and $\mu\nu$ events from CDF. The upper edge of the M_t distribution near M_W carries the bulk of the information used in fits. It can be broadened not only by the width of the W, but also by the finite detector resolution for electrons and neutrinos.

At this conference, Trivan Pal has presented a final UA2 result for M_W.[32] UA2 measures both M_W and M_Z, and relies on the more precise value of M_Z from LEP to define an energy scale. Without a precise value for M_Z, a scale uncertainty of order 800 MeV would result. Rather than quote M_W directly, they quote the more precise ratio of $M_W/M_Z = 0.8813 \pm 0.0036$ (stat) $\pm$ 0.0019 (syst),[32] which can be converted into M_W using the LEP value of $M_Z = 91.175 \pm 0.02$ GeV/c^2,[33] this can be translated into a value of $M_W = 80.35 \pm 0.33$ (stat) $\pm$ 0.17 (syst) GeV/c^2.

CDF's published result is a direct measurement of M_W and has a relatively small systematic uncertainty associated with absolute energy scale (0.1 % for muons and

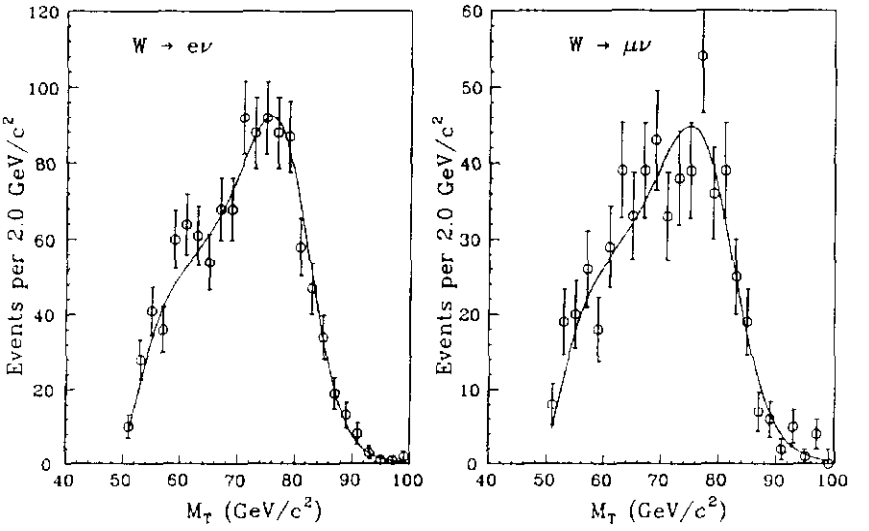

Figure 11: Transverse mass, M_t distributions of W's in $e\nu$ and $\mu\nu$ channels from CDF data.

0.2 % for electrons). This is largely a result of the ability to make an *in situ* calibration using the tracking in a solendoidal field, and checking the energy scale from the reconstructed J/ψ mass.[31] The statistical uncertainties are 350 MeV for electrons and 530 MeV for muons. The total systematic uncertainty is 240 MeV for electrons and 315 for muons. There is a common energy scale uncertainty of 80 MeV. The two largest uncertainties, of order 150 MeV are from the modeling of the W p_t resolution in the calorimeter, and the soft hadronic contributions. A high p_t Z sample can be used to check these effects, but has limited statistics. In addition, uncertainties in the proton structure function and backgrounds each add approximately 50 MeV. The combined muon and electron samples give $M_W = 79.91 \pm 0.39$ GeV/c^2, taking a fixed width of $\Gamma(W) = 2.1$ GeV.

The UA2 and CDF values of M_W can be averaged together to obtain 80.14 ± 0.27 GeV/c^2. It should be cautioned that the CDF and UA2 techniques for fitting the mass, and taking into account the transverse motion of the W are very similar for both experiments which probably introduces some correlation in the uncertainties. The LEP value of M_Z can be used in conjunction with this average to obtain an averaged $sin^2\theta_W = 0.2274 \pm 0.0052$.

Because the top is so much heavier than the other quarks, it plays a measurable role in electroweak radiative corrections. M_{top} enters into the mass difference of the W and Z^o due to $t - b$ loops present for the former, but not the latter. Figure 13 shows a plot of M_W versus M_t for different values of the Higgs mass.[34] The solid and dashed lines indicate the the current world averaged value of M_W and uncertainties. A value of M_t of $130\ ^{+40}_{-45}$ GeV/c^2 can be found, taking $M_{Higgs} = 100$ GeV/c^2, with an additional variation of $+30$ and -10 GeV/c^2 from the range $25 < M_{Higgs} < 1000$ GeV/c^2. A 95 % C.L. upper limit on M_{top} can be placed at 210 GeV/c^2 using $M_{Higgs} = 100$ GeV/c^2.

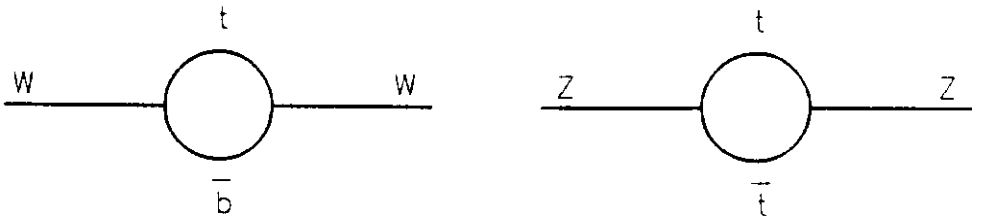

Figure 12: Electroweak loop diagrams illustrating the dependence of M_W/M_Z on M_t.

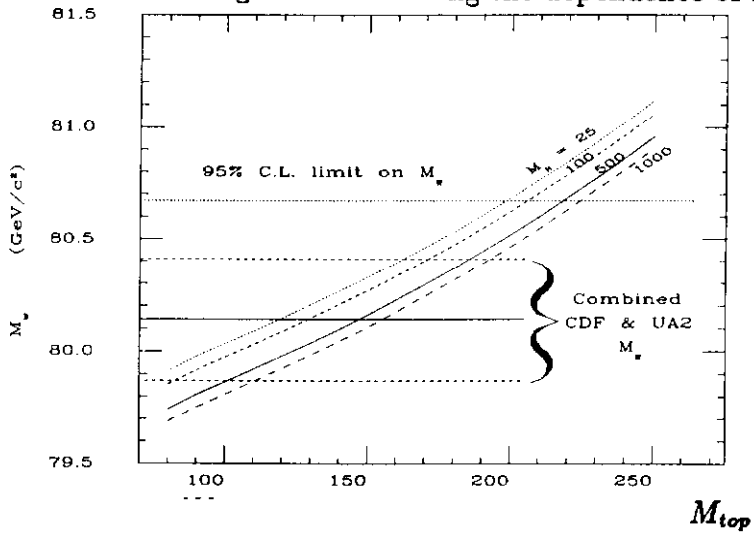

Figure 13: Relationship of M_W to M_t via electroweak radiative corrections. This uses the most recent LEP value of 91.175[33] for M_Z and the predictions of G. Degrassi *et al.*[34] for Δr. The world average of UA2 and CDF measurements for M_W is indicated.

From the figure, it is apparent that for an infinitely precise measurement of M_t, a precision of better than 50 MeV would be required to begin to constrain M_{Higgs}.

What is the ultimate precision of M_W from $\bar{p}p$ colliders? In the upcoming run of the Tevatron, a statistical error substantially less than 100 MeV/c^2 should be possible (see L. Nodulman's talk at this conference), at which point the measurement will be limited by systematic effects. These, too, may decrease as "control " data sets gain increased statistics (*e.g.* $Z \rightarrow e^+e^-$). On the other hand, backgrounds at high luminosity (*e.g.* event pile-up) may pose a problem. Assuming that the dominant uncertainties in the CDF analysis,[31] associated with the soft hadronic component can be reduced signficantly, then an uncertainty of 100 MeV/c^2 may be achievable.

3.2. $\Gamma(W)$

The width of the W, can be extracted with some precision from the ratio,

$$R \equiv \frac{\sigma(\bar{p}p \rightarrow W) \times Br(W \rightarrow l\nu)}{\sigma(\bar{p}p \rightarrow Z) \times Br(Z \rightarrow l\nu)} \tag{5}$$

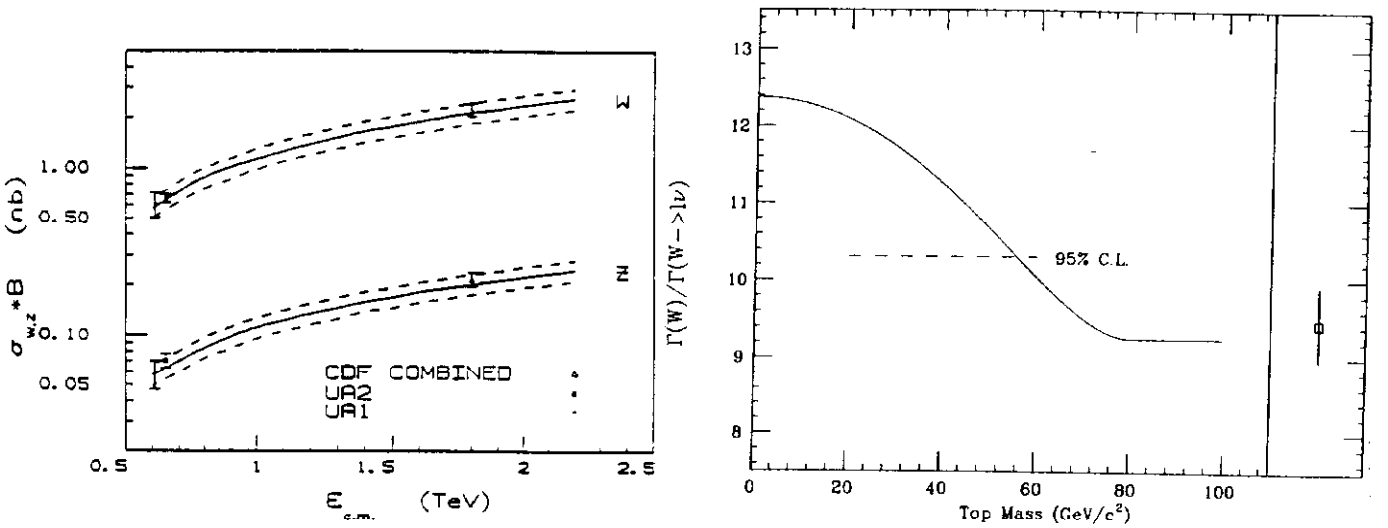

Figure 14: LEFT: Cross section times branching ratio for W and Z production reported by the UA1, UA2 ($\sqrt{s} = 0.63$) and CDF experiments (1.8 GeV) along with theoretical predictions. RIGHT: The average of UA1, UA2 and CDF values for $\Gamma(W)/\Gamma(W \to l\nu)$, along with the Standard Model prediction as a function of M_{top}.

as was pointed out by Cabibbo[35] and Halzen and Mursula.[36] By writing the branching ratios in terms of the partial widths, one finds

$$\Gamma(W) = \frac{1}{R}\frac{\sigma(W)}{\sigma(Z)}\Gamma(Z)\frac{\Gamma(W \to l\nu)}{\Gamma(Z \to l^+l^-)} \tag{6}$$

The first term is measured. The second is predicted by QCD, and, in taking the ratio of cross section, a large fraction of the uncertainties cancel. The third comes from LEP with high precision, and the fourth term can be derived using the electroweak relation

$$\frac{\Gamma(W \to l\nu)}{\Gamma(Z \to l^+l^-)} = \frac{M_W^3}{M_Z^3}\frac{2}{1 - 4sin^2\theta_W + 8sin^4\theta_W} \tag{7}$$

The cross sections times branching ratios for $\sqrt{s} = 1.8$ from CDF and 0.63 TeV from UA1 and UA2 are shown in figure 14, along with theoretical predictions.[37] The CDF data is a combination of e andμ channels. Unfortunately, the three experiments have independently calculated $\Gamma(W)$,[38,32,39] each using slightly different input assumptions for the ratios of the cross sections, partial widths and $\Gamma(Z)$. A direct world average of the reported values of $\Gamma(W)$ will neglect these differences, and also will combine systematic uncertainties which are highly correlated.

I will use the most recently available values of R: 9.98 $\pm$ 0.74 (CDF-e and μ) 10.4 $\pm$ 0.72 (UA2) 9.5 $\pm$ 1.05 (UA1) to extract $\Gamma(W)$ using a consistent set of inputs.

The ratio $\sigma(W)/\sigma(Z)$ is taken as 3.23 $\pm$ 0.05 for $\sqrt{s}$ = 1.8 TeV, and 3.16 $\pm$ 0.05 for 0.63 TeV,[37] where the uncertainty reflects variation with different choices of structure functions and uncertainties in M_W and M_Z. From LEP,[33] $\Gamma(Z)$ =2.487 $\pm$ 0.010 GeV; the ratio of the partial widths is taken from equation 6 using the most recent world averages. Putting it all together, one derives a world average for $\Gamma(W)$ = 2.14 $\pm$ 0.07 (stat +syst) $\pm$ 0.04 (theory), where the first error comes from taking the statistical and systematic errors on R as independent between the three experiments, and the last term is the correlated systematic coming mostly from the uncertainty on $\sigma(W)/\sigma(Z)$.

$\Gamma(W)$ is sensitive to the decay $W \rightarrow t\bar{b}$, independent of t decay mode, and can be used to set a lower limit to M_{top}. However, the ratio, $\Gamma(W)/\Gamma(W \rightarrow l\nu)$, is also sensitive to M_{top}, and allows one to use the more precise $\Gamma(Z \rightarrow l^+l^-)$ from LEP. With the same assumptions as above, this gives $\Gamma(W)/\Gamma(W \rightarrow l\nu)$ = 9.44 $\pm$ 0.44 (syst+stat) $\pm$ 0.16 (theory). Figure 14 shows this quantity, along with the standard model predictions as a function of M_{top}. From this figure, a lower limit of 55 GeV/c^2 can be placed on the top mass at the 95 % confidence level, which is independent of decay mode. The accuracy of $\Gamma(W)$, like M_W, is still statistics limited. With a higher yield of W's and Z's from the next run of the Tevatron Collider, a more precise value should be possible.

3.3. $W \rightarrow \tau\bar{\nu}_\tau$

SU(2) gauge invariance in the Standard Model implies a universality of lepton couplings to vector bosons. Measurements at LEP confirm this picture for neutral currents at approximately the 1 % level.[33] At hadron colliders, a similar test for charged currents is possible from the decay of W into $\tau + \nu_\tau$. Measurements of $\sigma \times Br(W \rightarrow \tau\nu_\tau)$ have recently been reported by both the CDF (see Aaron Roodman's talk, these proceedings) and UA2 Collaborations.[40] These can be used to derive fairly precise tests of universality for charged currents.

A τ decaying hadronically will give rise to a narrow, low multiplicity jet (1, 3 or 5 prong). The $W \rightarrow \tau\nu_\tau$ decay can also be identified by the large missing energy in the event. These two characteristics are sufficient to reduce the backgrounds from QCD jet production to a tolerable level. UA2 starts with an event sample triggered by a missing E_t requirement of 18 GeV, and makes an initial event selection requiring one cluster with $E_t > 22$ GeV and no other cluster with $E_t > 10$ GeV. In order to subtract out the large jet background, UA2 uses a Monte Carlo to determine a calorimeter energy profile and hadronic content expected for τ decaying in hadronic modes. Figure 15 shows one of these variables, ρ, which is the ratio of the sum of the energies in the two leading towers to the total energy in a cluster. τ decay products should be narrowly focused and hence have a value of ρ near unity, whereas the QCD background should be distributed more evenly. Using a Monte Carlo to predict the τ characteristics in these two variables allows UA2 to make a background subtraction to determine a cross section times branching ratio. From the ratio of $W \rightarrow \tau\nu_\tau$ to $W \rightarrow e\nu_e$, a test of universality can be made, giving[40] g_τ/g_e = 1.02$\pm$0.04 (stat.)$\pm$0.04(syst.).

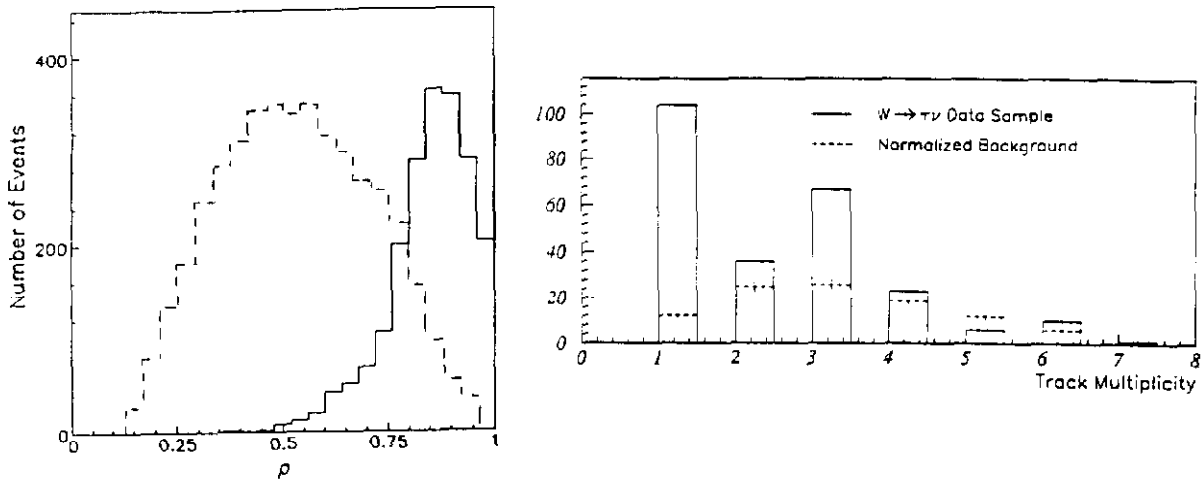

Figure 15: Distributions used to distinguish hadronic τ decays from the QCD background. RIGHT: ρ, employed by UA2 measures the narrowness of a jet (ρ =1 implies a narrow jet). The solid line indicates the expected shape of ρ from τ decays, while the QCD background is shown as the dotted line. RIGHT: is the distribution of charged tracks associated with a τ cluster from CDF data. The excess of 1 and 3 prong events identifies the τ signal.

CDF's data sample comes from two independent triggers, each employing a missing E_t requirement; one requires a minimum missing E_t of 25 GeV, and an cluster with more than 8 GeV of EM energy. The second trigger requires a missing E_t >20 GeV and a narrow cluster (2 towers) with E_t >10 GeV, and a stiff track pointing at it. In event reconstruction, the charged multiplicity of the τ cluster is defined as the number of stiff tracks in a 10° cone around the cluster with $p_t > 1.0$ GeV/c. A seed track with $p_t > 5$ GeV/c is required. An isolation requirement is made by asking that no tracks be in a region between 30° and 10° around the τ cluster. After the isolation requirement, a plot of the multiplicity of tracks with $p_t > 1$ GeV/c shows a distinct signal as an excess of 1 and 3 tracks pointing at the cluster (Figure 15). After a background subtraction is made from a non-isolated sample CDF find: g_τ/g_e =0.97 ± 0.07. From CDF, UA2 and the older UA1 result[41] (1.01±0.09±0.05), a world average of 0.99 ± 0.04 is obtained.

4. Heavy Quark Production

4.1. Inclusive b-quark Production

A measurement of the cross section for the inclusive production of b quarks at $\overline{p}p$ colliders is well motivated:

1. It provides an important check of QCD calculations.

2. It is sensitive to the gluon distribution at low x, for which there are only limited measurements.

3. It is an important "engineering" number which allows one to predict yields for studies of weak decay parameters (*eg* CP violation).

At present, a prediction exists at $\mathcal{O}(\alpha_s^3)$ for the inclusive cross section $\sigma(\overline{p}p \rightarrow b + X)$.[42] These predictions are evaluated for cuts appropriate to both the CDF[43] and UA1 experiments.[44] Unlike the QCD predictions for jet production (see earlier section), the theoretical uncertainty has, if anything, become larger at $\mathcal{O}(\alpha_s^3)$. At $\sqrt{s} = 1.8$ TeV, the theoretical uncertainty is approximately 60 %.

UA1 and CDF select b's from lepton triggers. These lepton can be produced near hadronic energy associated with jets. This additional energy can be used to separate out b from c and W,Z production. The UA1 experiment uses muons exclusively to tag b quarks[44] because they can be detected inside relatively dense hadronic jets. From a Monte Carlo simulation, the charm background can be identified and subtracted from the p_t^{rel} distribution, the angle between the muon and jet axis. UA1 has also used dimuon data to extract low p_t measurements.

The CDF experiment has used a sample of inclusive electrons to obtain a b cross section.[43] This method has the drawback that in order to trigger and identify the electrons, some implicit isolation of the electron is required, reducing the acceptance for b's substantially above 40 GeV due to associated hadronic activity. In addition, CDF has a signal for B$\rightarrow$ K$^{\pm}J/\psi$ and K$^{*o}J/\psi$ (see below), which can be used to extract a low p_t datum.

For both experiments, the charm contributions are estimated to be relatively small, and is determined via Monte Carlo. Figure 16 shows both the CDF and UA1 inclusive b cross sections along with the predictions of Nason, Dawson and Ellis.[42] The cross sections are displayed as a function of the integrated value above some fixed p_{tmin}, hence the errors are strongly correlated from bin to bin. The dashed lines indicate the theoretical uncertainties. The UA1 data appear to be consistent with the central value of the calculation, while the CDF data appear to be systematically high. It is curious that one is in agreement with the central theoretical value and the other is high. One possible explanation lies in different regions of x probed by the two experiments. There is some expectation that large higher order contributions in the lower x region probed by CDF might explain the result.[45–47]

4.2. Charm and Bottom Decays

Until recently, the reconstruction of exclusive decays of B mesons was restricted to e^+e^- experiments with $\sqrt{s}$ in the Υ region.[48] The CDF collaboration has reported a signal for $B \rightarrow J/\psi\, K^{\pm}$ and $J/\psi\, K^{*o}$. The combined K^{*o} and $K^{\pm}$ signals are shown in figure 17. A fit to the data give a mass of 5.279$\pm$0.006 GeV, consistent with ARGUS and CLEO measurements.

Although the cross sections for bottom and charm are higher at hadron colliders than e^+e^- machines, the production mechanisms are significantly more complicated. CDF, however, has begun an exploration of resonances associated with electron and J/ψ production. Although these results are only qualitative at the moment, they demonstrate that there is wealth of information that can be used to disentangle the

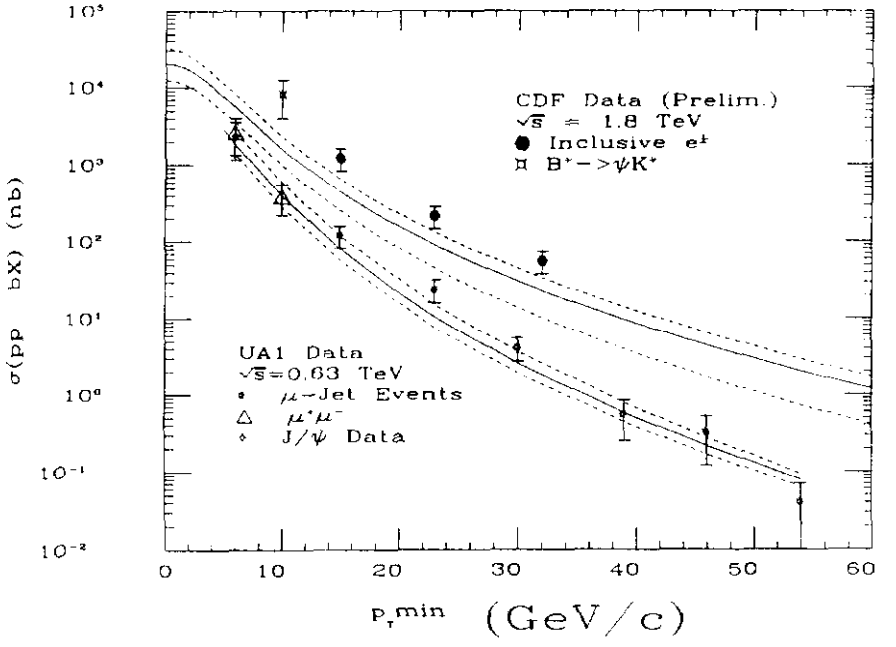

Figure 16: The inclusive b cross section, plotted as an integral above a fixed value of p_{tmin}. The data are from the UA1 and CDF experiments at $\sqrt{s} = 0.63$ and 1.8 TeV. Also shown are the predictions of Nason, Dawson and Ellis.[42]

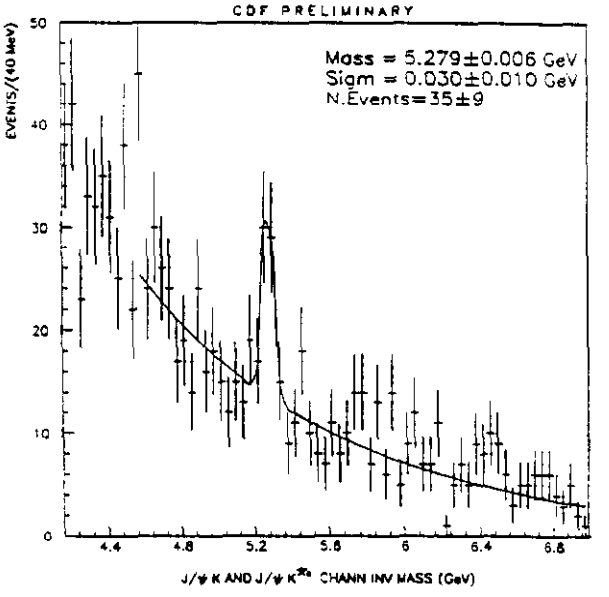

Figure 17: Reconstruction of $B \to J/\psi + K^{\pm}(K^{*o})$ in the CDF detector.

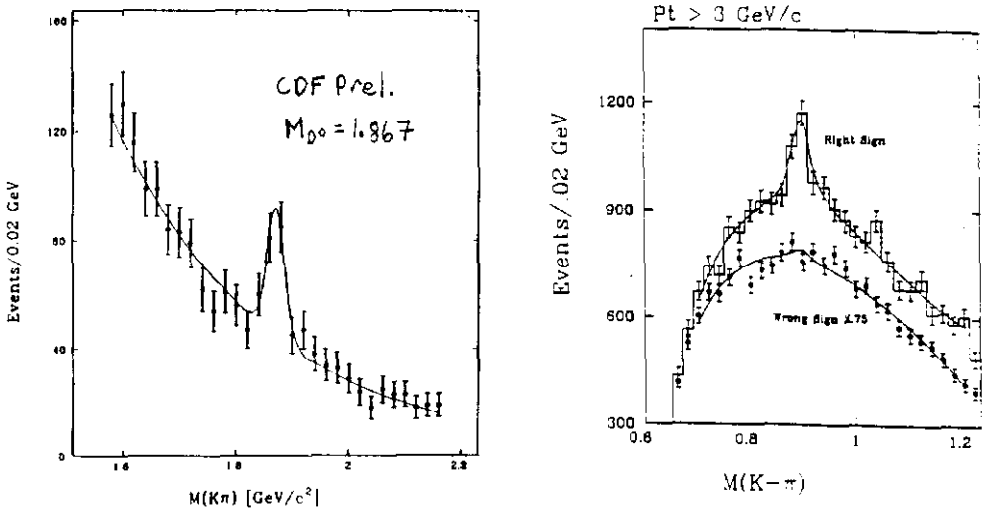

Figure 18: Signal for D^o for same sign combinations of e and K in the CDF inclusive electron sample. No signal in the opposite sign combination is observed. Also shown is the K^{*o} peak associated with same sign $e-K$ combinations and no signal seen in the opposite sign combination.

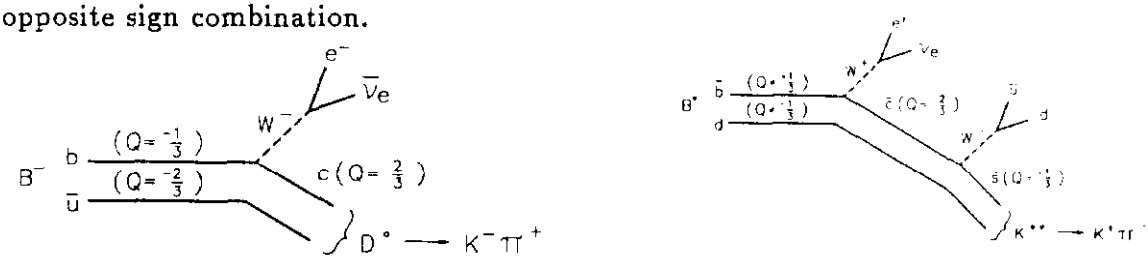

Figure 19: Diagrams illustrating the source of e, K sign correlations from B decays giving rise to D^o and K^{*o}.

signals. As an example, figure 18 shows a D^o signal associated with the inclusive electron sample described in the previous section. The fact that a D^o signal appears where the K and e charges are the same sign but not when they're opposite is evidence favoring the predominance of b production in this sample. Similarly, a K^{*o} signal is seen in conjunction with the CDF electron data (figure 18), where the combination consistent with B production is seen ($e^+K^{*o}(K^+\pi^-)$) but not the opposite sign combination ($e^+\overline{K^{*o}}(K^-\pi^+)$). If charm pair production were the source of the electrons, then one would expect roughly equal numbers in the same sign (K+e charges correlated) and opposite sign combinations. This is illustrated in figure 19.

Direct J/ψ production is expected to suppressed because direct production proceeds via a three gluon vertex.[49] The bulk of J/ψ's produced are expected to come from the decays of b's and χ's. Figure 20 shows a signal for χ production in the $\gamma\, J/\psi$ final state. The fraction of J/ψ's that come from χ decays is 37 ± 7 (stat)±11 % (syst). This number also includes sequential decays from $B \rightarrow \chi + X$. The fraction of J/ψ's coming from direct B decays has been estimated at 64 ± 28 %.[50]

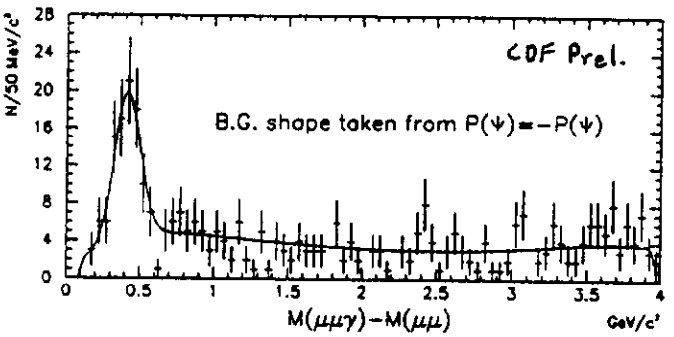

Figure 20: χ signal in $\gamma\, J/\psi$ final state, from CDF.

4.3. B^o,$\overline{B}^o$ Mixing

B^o, $\overline{B}^o$ mixing provides information about the Cabbibo, Kobayashi, Maskawa (CKM) matrix elements. In figure 21, the box diagrams taking B^o into $\overline{B}^o$ are shown. The exhange of t dominates, hence measurements of mixing gives information on the CKM elements $|V_{td}|^2$ and $|V_{ts}|^2$. Because the far off-diagonal elements of the CKM matrix are small, B_s,$\overline{B}_s$ mixing is expected to be larger than B_d,$\overline{B}_d$ mixing.

In $\overline{p}p$ colliders, both B_s,$\overline{B}_s$ and B_d,$\overline{B}_d$ mixing occur. One can describe the mixing in terms of the $\chi_{d(s)}$ parameter defined by:

$$\chi_{d(s)} \equiv \frac{\mathcal{P}(B^o_{d(s)} \to \overline{B}^o_{d(s)})}{\mathcal{P}(B^o_{d(s)} \to B^o_{d(s)}) + \mathcal{P}(B^o_{d(s)} \to \overline{B}^o_{d(s)})} \tag{8}$$

In both CDF and UA1, the measured quantity is:

$$\overline{\chi} \equiv \frac{\mathcal{P}(b \to \overline{B}^o \to B^o \to l^+)}{\mathcal{P}(b \to l^\pm)} = f_d\chi_d + f_s\chi_s \tag{9}$$

where $f_d(f_s)$ is the product of cross section times branching ratio to leptons for $B^o_d(B^o_s)$ divided by the same quantity for all hadrons containing b quarks.

UA1[51] has measured $\overline{\chi}$ for dimuon events and obtained $\overline{\chi} = 0.158 \pm 0.059$. CDF has used both e,μ and e,e events to determine $\overline{\chi}$ and obtains from the combined sample $\overline{\chi} = 0.176 \pm 0.031$ (stat+syst) $\pm$ 0.032 (MC).[43] The primary advantage of $e-\mu$ mixing is the absence of backgrounds from Drell-Yan and J/ψ decays. These measurements can be combined for a world average of 0.170 ± 0.036. Figure 21 shows the combined CDF and UA1 result in a plot of χ_d versus χ_s along with the combined result from CLEO and ARGUS.[52] The slope of the line from the collider results uses $f_d = 0.375$ and $f_s = 0.15$ to account for the relative fraction of down and strange quark production. The hatched area indicates the region allowed by the standard model.

4.3.1. Prospects for b Physics at $\overline{p}p$ Colliders

In the upcoming run of the Tevatron Collider, one can expect upwards of 100 pb^{-1} on tape. This by itself should give a twentyfold increase in the number of b's on tape. With

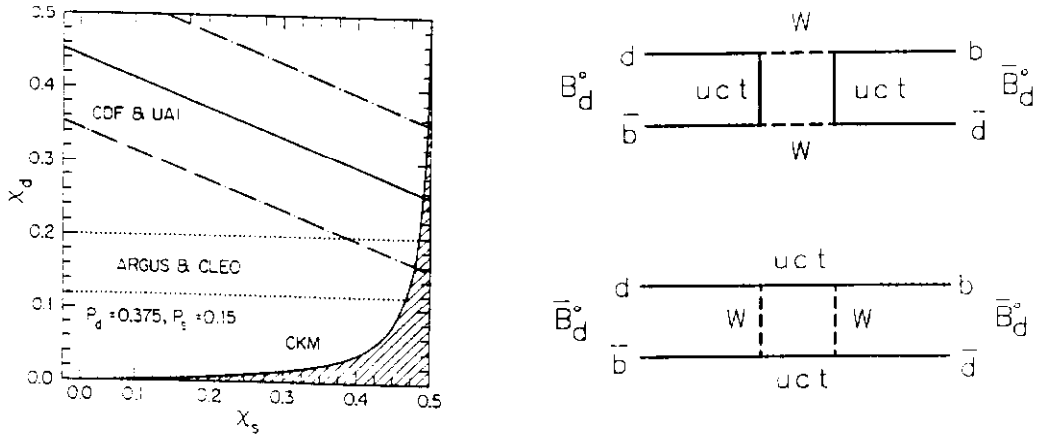

Figure 21: Results from CDF, UA1 and ARGUS on b mixing, showing the results in terms of χ_s and χ_d. The hatched area shows the region allowed by the standard model. On the right are the box diagrams contributing to $B^o - \overline{B}^o$ mixing.

improvements in the CDF triggering, an extrapolation of the current $B \rightarrow J/\psi K^{\pm}(K^{*o})$ signal implies something the order of 3000 events in this channel. These may have a tag in a new silicon vertex detector, which has a resolution approximately 25 μm. In addition, the prospects are good for finding $B_s \rightarrow J/\psi + \phi$. If this is found, then a large number of possibilities are opened up for exploring the CKM matrix elements, including species dependent lifetimes and mixing. Finally, the prospect of a measurement of CP violation in the b system remains a possibility at the Tevatron with the Main Injector.[54]

4.4. Limits on Top Production from $\bar{p}p$ Colliders

Heavy top is expected to be produced in $\bar{p}p$ collisions via $\bar{p}p \rightarrow \bar{t}t + X$, where t then decays into Wb. Depending on the top mass, the W can be real or virtual. The W then can decay into a $\bar{q}q$ pair, or $l\nu$. Because of potential QCD backgrounds, and because of the poorer calorimeter resolution for jets, search modes for top are in the channels where one or both W ' s decay into a lepton. The dilepton mode is the cleanest, but has the smallest branching fractions (2/81 for $e\mu$, and 1/81 for ee or $\mu\mu$). The channel for $\bar{t}t$ into leptons plus jets has a larger branching fraction, but there is a substantial contribution from high p_t W production.

Limits from the S$\bar{p}p$S collider experiments UA1 and UA2 have not changed since 1990, results can be found in references in the bibliography.[56,57] At present, the most stringent limit on M_t assuming standard model decays comes from the CDF experiment with an integrated luminosity of 4.2 pb^{-1}. It is the result of combining $e\mu$ ee, $\mu\mu$ channels and looking for W plus jets where one of the jets has a soft μ from b decays. Details of this analysis can be found in the talk by T. Liss at this meeting. Leptons are required with $p_t \geq 15$ GeV in the central pseudorapidity region. The most crucial cuts require the leptons to not be back-to-back ($20^o < \Delta\phi_{ll} < 160^o$), and the dilepton invariant mass not be in a window associated with the Z^o ($75 < M_{ll} < 105$ GeV/c^2). After imposing these cuts, only one $e\mu$ event remains,[58] which is consistent with an

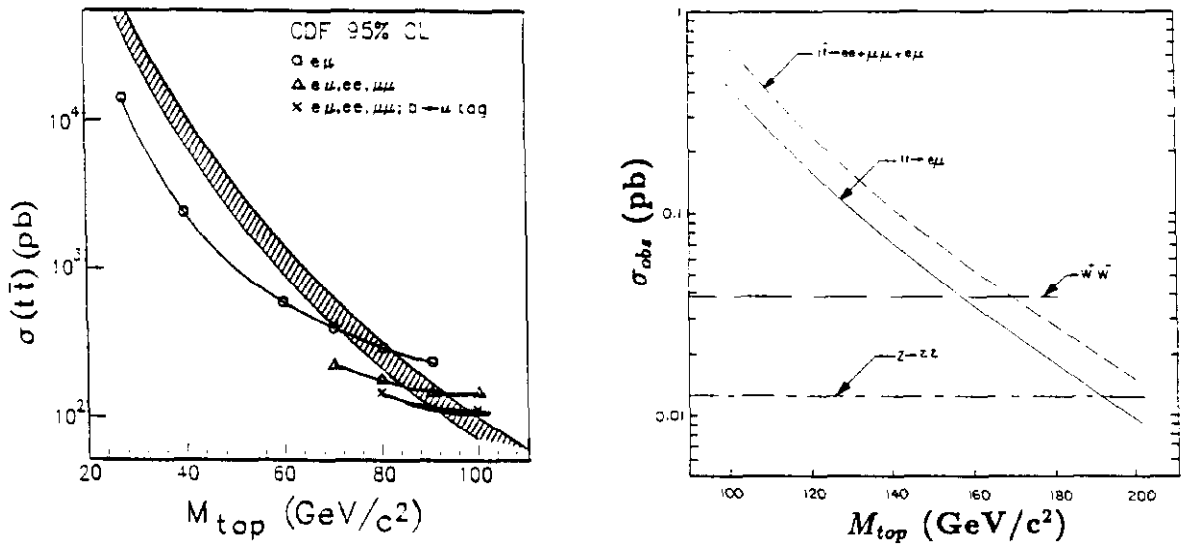

Figure 22: LEFT: 95 % C.L. limit on M_t set at 89 GeV/c^2 by CDF. The limit is derived from the intersection of the 95 % C.L. limits on the cross section with the theoretical prediction plus uncertainty (band). RIGHT: Cross section times acceptance for dilepton events in the CDF detector for heavy M_{top}.

expected background of 1.5 events from a variety of processes (*e.g.* $Z^o \rightarrow \tau\tau, \bar{b}b$). The efficiency for the dilepton channel is approximately 16 %.

In the lepton plus jets channel, an isolated μ or e is required with $p_t > 20$ GeV/c, a missing E_t greater than 20 GeV, and a minimum of 2 jets with $E_t > 10$ GeV, and $|\eta| \leq 2.0$. 104 $e + jets$ and 91 $\mu + jets$ events remain. If $\bar{t}t \rightarrow Wb + Wb$ were a source of these events, one expects a sizable fraction of the b quarks to decay into a μ. With the requirement that there be a μ with $p_t > 2$ GeV/c, and the μ be at least 0.5 units of ΔR away from the two most energetic jets, no events remain.

By combining all sets of data, and using the ISAJET simulation[59] to predict the acceptance as a function of top mass, the 95 % C.L. limit on $\sigma(\bar{t}t)$ can be plotted. This is shown in figure 22 for each of the processes. Where the curves intersect the lower limit of the theory cross section a limit on the top mass can be derived which takes into account the theoretical uncertainty. This is now 89 GeV/c^2 from CDF data. It should be pointed out out that these limits are not valid for models in which top does not decay with standard couplings (*e.g.* charged Higgs).

4.5. Prospects for Finding Top

Because of the small backgrounds, the dilepton channels, particularly the $e\mu$ channels are the ideal discovery channels. Figure 22 shows the cross section[64] times a 16 % acceptance for lepton pairs (in the above analysis). There is also indicated the background from W pair production, which becomes significant for very heavy top.[61] By 1994, the Tevatron Collider should accumulate approximately 100 pb^{-1} of data. This would give a reach of approximately 170 GeV for a small visible excess ($\approx$ 4

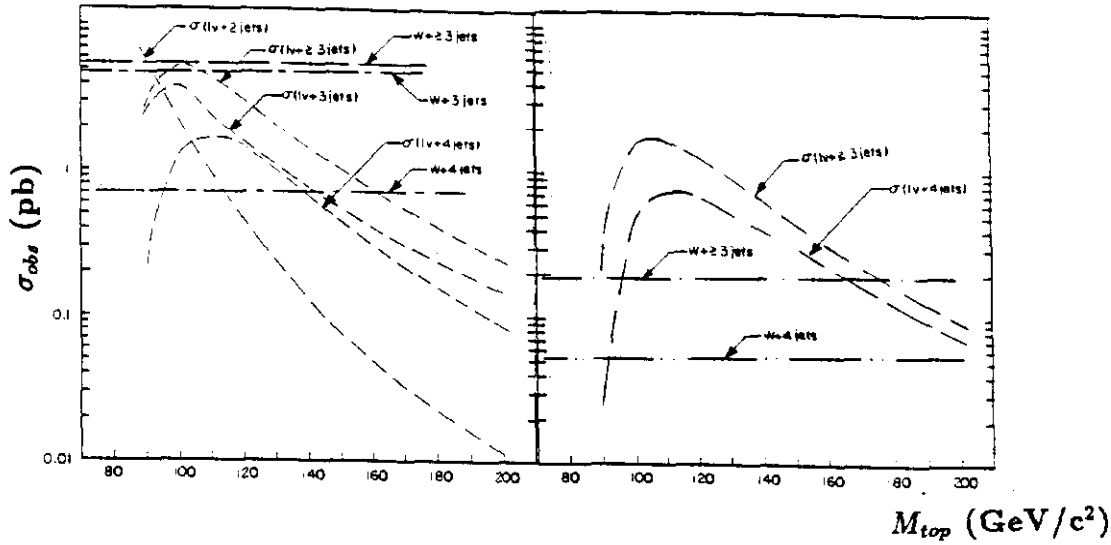

Figure 23: LEFT: Cross sections for $t\bar{t} \rightarrow l\nu + n$ jets as a function of top mass The background from $W + n$ jets is also shown..[20] RIGHT: Same processes, but with the addition of a b tag to reduce backgrounds.

events) in the dilepton channel. From the rate of dilepton production, one can get a crude estimate of the top mass. This is limited due to theoretical uncertainties in the parton distribution functions and the contribution of higher order contributions which have not been evaluated.[64] An accuracy of about 20 GeV might be possible from the rate alone.

The discovery of an excess of dilepton events may signal a discovery of top, but it doesn't fully demonstrate that the excess is caused by top (*e.g.* as opposed to an anomalous rate of W pair production). In order to prove that top is being produced, one must demonstrate its couplings and that it decays to Wb. The channel involving leptons plus jets is the most promising for this kind of detailed study. Although the rates are higher than the dilepton channel, the main disadvantages to using leptons+jets is the expected background from high P_t W production, and the poorer resolution associated with jets.

Figure 23 shows the cross sections expected for $W + n$jets as background and the yield of top going into $l\nu + n$ jets.[63] The curves were generated by assuming reasonable cuts on minimum jet and lepton E_t (15, 20 GeV) and maximum pseudorapidity: $|\eta_{max}|$ <2.0, 1.0 for jets and leptons respectively.[63] As the mass of top increases, the 4th jets becomes easier to identify, but the signal to noise is also getting worse. Again, this illustrates the need for b tagging to reduce the backgrounds. If a b tag is used, an efficiency of approximately 50 % is introduced, however the corresponding background from $W + n$jets is significantly reduced. This is shown in figure 23.

After the discovery of top, it would take a substantial yield of events to generate proof of the $t \rightarrow Wb$ decay mode. Figure 24 shows the invariant mass distributions for two and three jet combinations showing both a top signal in the three jet combinations

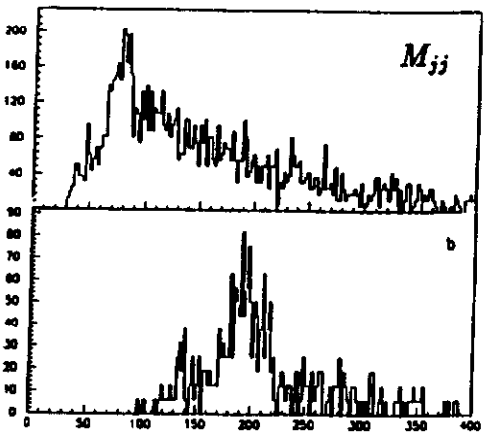

Figure 24: Possible experimental signatures for top in the two and three jet invariant mass distributions, with M_t = 200 GeV/c², after the addition of a vertex tag.

where the two jet combinations are constrained to be within ± 20 GeV of the W mass.[65] After employing a b tag, there are clear peaks signaling the W in M_{jj} and for the top in M_{jjj}. The precision that one might expect in the mass measurement may be of order 8 GeV/c, limited by systematic uncertainties on the calorimeter response, and the modeling of various physics processes, such as gluon bremstrahlung. To reach a stage where the statistical uncertainty is less than the systematics for this type of analysis, one might require of order 300 top events with $l + \nu + 4$jets. This corresponds roughly to 250 pb^{-1} for M_t = 130 GeV/c².

5. Exotics

5.1. Compositeness

If quarks and/or leptons had a substructure, then one might expect on general grounds a binding force of the constituent particles that would become evident only at very short distances. One can parameterize the possible effects of compositeness in terms of a 4-Fermi term to be added to the Lagrangian. In the case of $q\bar{q} \rightarrow q\bar{q}$ scattering, this is:

$$\mathcal{L}_{comp} = \frac{g^2}{2\Lambda_{qc}^2}(\bar{q}\gamma_\mu q)^2 \qquad (10)$$

Here the constant Λ_c has the units of energy, and characterizes the scale at which the quarks have substructure. The consequences of adding this to the QCD Lagrangian is to increase the rate of jet production at high E_t. From shape of the inclusive jet cross section at high E_t. A limit on Λ_c has been set at 825 GeV (95 % C.L.) by the UA2 collaboration,[16] and at 1.4 TeV (95 % C.L.) by the CDF collaboration. These both assume a unity strength coupling ($g^2 = 4\pi$). This says that quarks are pointlike objects down to 1.4 × 10^{-17} cm.

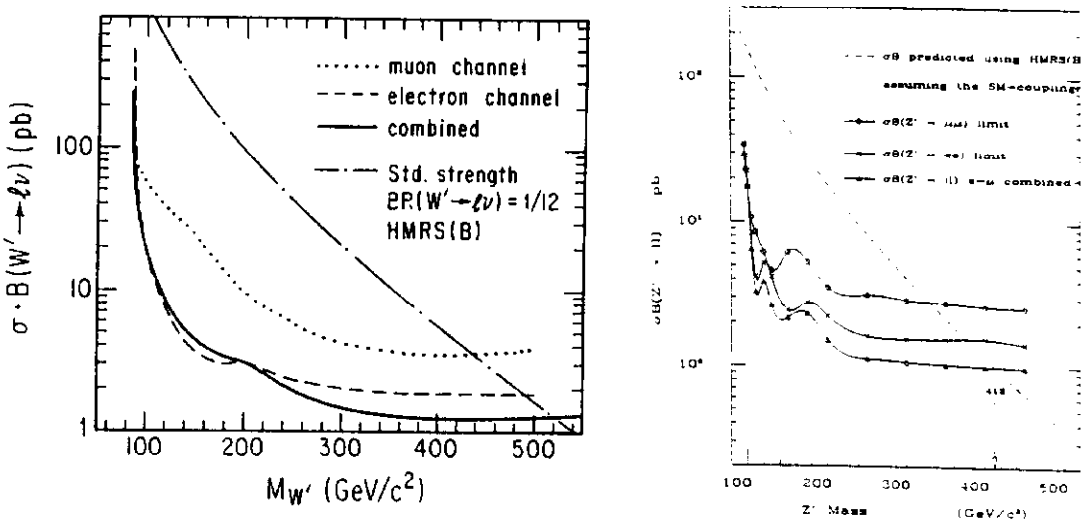

Figure 25: Limits on cross section times branching ratio for heavy W and Z bosons.

A similar term can be introduced to test quark-lepton compositenss:

$$\mathcal{L}_{comp} = \frac{g^2}{2\Lambda_{lc}^2}(\bar{l}\gamma^\mu l)(\bar{q}\gamma_\mu q) \tag{11}$$

This term would be manifest as an excess in Drell-Yan ($\bar{q}q \rightarrow l^+l^-$) production at high dilepton invariant mass. CDF has measured Drell Yan production at high p_t, and is able to set a lower limit on Λ_{ec} at 1.7 TeV and $\Lambda_{\mu c}$ at 1.3 TeV (95 % C.L.).

5.2. Heavy Gauge Bosons

Heavy guage bosons can arise in many extensions of the Standard Model. A heavy Z boson would appear as bump in the invariant mass invariant mass distribution for Drell-Yan pairs. CDF has searched for an excess of either dimuon or di-electron pairs at high M_{ll}, and found no significant excess (see talk by T. Fuess at this conference). From this a lower limit can be set (figure 25), assuming standard model couplings, of $M(Z') > 412$ GeV/c^2 (95 % C.L.).

Similarly, a heavy W boson could appear as an excess in the lepton-neutrino transverse mass distribution. Again, CDF has used a combined sample of electrons and muons to derive a limit on heavy W's. Figure 25 shows the limits on the cross section times branching ratio for W'. Assuming a standard coupling, a lower limit can be set at 520 GeV/c^2 (95 % C.L.).

5.3. Supersymmetry

Expected signatures of supersymmetry at hadron colliders depend the relative masses of the squark, gluino and photino. Expected decay modes for squarks and gluinos are $\tilde{g} \rightarrow \bar{q}q\tilde{\gamma}$, $\tilde{q} \rightarrow q\tilde{g}$ and $q\tilde{\gamma}$, depending on their relative masses. In all cases, if squarks or gluinos were being produced, one would expect to observe events with

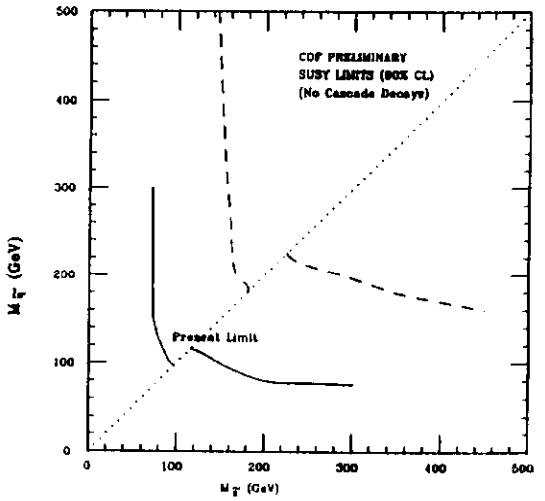

Figure 26: Limits on the masses of squarks and gluinos from the CDF detector.

jets and a large missing E_t. CDF[66] has searched for events with 2 jets with $E_t > 15$ GeV and a missing $E_t > 100$ GeV; sensitive to the case where $M(\tilde{q}) < M(\tilde{g})$. Three events were observed with an expected background of 1.3 events. For the case where $M(\tilde{g}) < M(\tilde{q})$, four jets with $E_t > 15$ GeV were required with a missing $E_t > 40$ GeV. Two events were observed, again with an expected background of 1.3 events. These results can be turned into limits on squark and gluino masses, which is plotted in figure26.

6. Summary

To summarize, in the last year we have seen many of the final results from the S$\bar{p}p$S Collider, and have indications of good prospects for top at the Tevatron Collider. In elastic scattering, an average of E710 and CDF measurements of $\sigma_{tot} = 72.1 \pm 2$ mb is consistent with extrapolations from lower energies. A new ρ value, expressing the ratio of the real to the imaginary scattering amplitude at $t = o$, has been reported by E710: 0.13 ± 0.7, which is consistent with measurements made below S$\bar{p}p$S energies, but not of sufficient precision to be in contradiction with the anomalous UA4 result.

The quality of the comparison of jet data with QCD has improved with smaller systematics and improved theoretical uncertainties; the shape of high E_t jets is well described at the level of a single gluon bremsstrahlung. Tree level predictions give a good description of the topology of three jet events, but have relatively large uncertainties when applied to cross sections (UA2 and CDF). Direct photon and high p_t W, Z production are well described by next-to-leading order QCD predictions. UA2 has measured $\alpha_s = 0.123 \pm 0.025$ from W plus jet events.

The precision of measurements of M_W and $\Gamma(W)$ are still limited by statistics. Results from UA1, UA2 and CDF with final data sets can be averaged to obtain $M_W = 80.14 \pm 0.27$ GeV/c^2, and $\Gamma(W) = 2.14 \pm 0.08$ GeV. In combination with the

LEP value for M_Z, one finds $sin^2\theta_W = 0.2274\pm0.0052$. From the averaged ratio, $\Gamma(W)/\Gamma(W \rightarrow l\nu)$, a limit on M_{top} can be set at 55 GeV/c^2, independent of decay mode. From M_W and electroweak radiative corrections, an upper limit on M_{top} can be set at 210 GeV/c^2, with a central value of 130$\pm$40 GeV/c^2 (assuming M_{Higgs}=100 GeV/c^2). Two new measurements of τ universality from $W \rightarrow \tau\nu$ from UA2 and CDF can be combined with a UA1 measurement to form the average $g_\tau/g_e = 0.99 \pm 0.04$.

The averaged value for the B mixing parameter $\overline{\chi}$ from UA1 and CDF gives 0.17$\pm$0.04. The inclusive b cross section from CDF is slightly higher than theoretical predictions, but the UA1 result is in perfect agreement with QCD. The prospects for the discovery of top in future runs of the Tevatron Collider are good, but the backgrounds from W pair production and high p_t boson production are serious, especially for a very heavy top.

Finally, searches for exotic particles continue to produce null results but do extend limits on the point-like nature of quarks ($< 1.4 \times 10^{-17}$ cm), masses of heavy Z' and W' ($M_{Z'} > 412$ GeV/c^2, $M_{W'} > 520$ GeV/c^2). Limits on supersymmetry have also been extended.

7. Acknowledgements

I would like to thank in advance the organizers of this conference for their hospitality (this manuscript was prepared before the conference). I am grateful to Steve Ellis, Sarah Eno, Zoltan Kunszt, Michelangelo Mangano, Paolo Nason, Theresa Rodrigo, David Smith, Davison Soper and Darien Wood for their help with various questions I had in the preparation of this paper.

References

1. D. Bernard *et al.* (UA4 Collaboration), Phys. Lett. **B 198** 583 (1987).
2. D. Bernard, P. Gauron, B. Nicolescu, Phys. Lett. **199B** 125 (1987).
3. S. White, (CDF Collaboration) Proceedings of the 4th International Conference on Elastic and Diffractive Scattering La Biodola, Elbe, Italy, 22-25 May 1991, to be Published in Nucl. Phys. **B** (1991).
4. S. Shukla, (E710 Collaboration) Proceedings of the 4th International Conference on Elastic and Diffractive Scattering La Biodola, Elbe, Italy, 22-25 May 1991, to be Published in Nucl. Phys. **B** (1991).
5. M. M. Block, and R.N. Cahn, Phys. Lett. **B188**, 143 (1987).
6. P. Aurenche *et al.*, Phys. Rev. **D39** 3275 (1989).
7. P. Harriman, A. Martin, R. Roberts and W. Stirling, Rutherford Laboratory Preprint RAL-90-007 (1990).
8. J. Morfin and W.K. Tung, Fermilab Preprint Fermilab-Pub-90/74 (1990).
9. R. Ellis and J. Sexton, Nucl. Phys. **B 269** 445 (1986).
10. F. Aversa *et al.* , Phys. Lett. **B210** , 225 (1988).
11. S. Ellis, Z. Kunszt and D. Soper, Phys. Rev. Lett., **62** 2188 (1989); Phys. Rev. Lett. **64** 2121 (1990).

12. J. Huth *et al.*, published in "Proceedings of the 1990 Summer Study on High Energy Physics - Research Directions for the Decade ", Snowmass, Colorado, June 25 - July 13, 1990, Ed. E. Berger; preprint Fermilab CONF-90/249-E (1990).
13. F. Abe *et al.* (CDF collaboration), Phys. Rev. Lett **62**, 613 (1989).
14. J.A. Appel *et al.*, (UA2 Collaboration) Phys. Lett. **B160** 349 (1985).
15. G. Arnison *et al.* (UA1 Collaboration), Phys. Lett. **B 177** 244 (1986).
16. J. Alitti *et al.* (UA2 Collaboration), Phys. Lett. **B 257** 232 (1991).
17. S. Ellis, Z. Kunszt and D. Soper, Private Communication.
18. G. Marchesini and B.R. Webber, Nucl. Phys. **B310**, 461 (1988).
19. F. Abe *et al*, (CDF Collaboration), Fermilab Preprint Fermilab PUB-91/181, submitted to Phys. Rev. D (1991).
20. Z. Kunszt, E. Pietarinen, Nucl. Phys. **B164** 45 (1980); T. Gottschalk, D. Sivers, Phys. Rev. **D 21** 102 (1980); F. Berends *et al* , Phys. Lett. **118 B** 124 (1981).
21. M. Mangano and S. Parke, Phys. Rep. **200** 303 (1991).
22. G. Martinelli, plenary talk presented at the 1991 International Lepton-Photon Symposium, Geneva, Switzerland, 25 July-1 August 1991.
23. P. B. Arnold, M.H. Reno, Nucl. Phys. **B319**; P.B. Arnold and R.P. Kauffman, Nucl. Phys. **B349**, 381 (1991).
24. F. Abe, *et al.* (CDF Collaboration), Phys. Rev. Lett. **66** 2951 (1991).
25. F. Abe, *et al.* (CDF Collaboration), FERMILAB-PUB-91/199-E, submitted to Phys. Rev. Lett. (1991).
26. J. Alitti *et al.* (UA2 Collaboration), CERN-PPE/91-68 submitted to Phys. Lett. (1991).
27. P. Aurenche, *et al.*, Phys. Rev. **D 42**, 1440 (1990).
28. E. Berger, talk presented at this conference.
29. H. Baer, J. Ohnemus, and J.F. Owens, Phys. Lett. **B234**, 127 (1990).
30. W.J. Marciano, and A. Sirlin, Phys. Rev. **D 29**, 945 (1984).
31. F. Abe *et al.* (CDF Collaboration), Phys. Rev. **D 43**, 2070 (1991).
32. Trivan Pal,(UA2 Collaboration) talk presented at this conference.
33. Janet Carter, Plenary talk given at the Lepton-Photon Symposium, 25 July-1 August 1991, Genveva Switzerland.
34. G. Degrassi, Fanchiotti, Sirlin, Nucl. Phys. **B 351** 49 (1991).
35. N. Cabibbo, "Proceedings of the Third Topical Workshop on Proton-Antiproton Collider Physics", CERN 83-04, 567, (1983).
36. F. Halzen and K. Mursula, Phys. Rev. Lett. **51**, 857 (1983).
37. A.D. Martin, W.J. Stirling, and R.G. Roberts, Phys. Lett. **B228**, 149 (1989).
38. C. Albajar, *et al* (UA1 Collaboration), Phys. Lett. **B253**, 503 (1991).
39. F. Abe, *et al.* (CDF Collaboration), Phys. Rev. **D 44**, 29 (1991).
40. J. Alitti, *et al.* (UA2 Collaboration), CERN-PPE/91-69, submitted to Z. Phys. **C** (1991).
41. C. Albajar, *et al.*, (UA1 Collaboration), Phys. Lett. **B185**, 233 (1987).
42. P. Nason, S. Dawson and R.K. Ellis, Nucl. Phys. **B 303** 607 (1988); **B 327** 49 (1989); **B 335** 260 (1990).

43. A. Sansoni (CDF Collaboration), to be published in "Proceedings of the 25^{th} Rencontres de Moriond", 17-24 March 1991, Les Arcs, France (1991).
44. C. Albajar *et al.* (UA1 Collaboration), Phys. Lett. **B 256** 121 (1991).
45. S. Catani, M. Ciafaloni and F. Hautmann, Phys. Lett. **B 242** 97 (1990).
46. E. Levin, DESY Preprint DES-91-054 (1991).
47. J. C. Collins and R.K. Ellis, Fermilab Preprint Fermilab-PUB-91/22-T (1991).
48. *c.f.* E.H. Thorndike and R.A. Poling, Phys. Rep. **157** 183 (1988).
49. N. Glover *et al.*, Z. Phys. **C38**, 473 (1988).
50. L. Pondrom, FERMILAB-Conf-90/256-E, to be published in the proceedings of the XXVth Int. Conf. on High Energy Physics, Kent Ridge, Singapore, August 2-8 1990 (1990).
51. H.C. Albajar, *et al.* , CERN-PPE/91-55, submitted to Phys. Lett. (1991).
52. H. Albrecht, *et al.*(ARGUS Collaboration), Phys. Lett. **B 192**, 245 (1987).
53. M. Artuso, *et al.* (CLEO Collaboration), Phys. Rev. Lett. **62** 2233 (1989).
54. C.S. Kim, J.L. Rosner, and C.P. Yuan, Phys. Rev. **D 41**, 1522 (1990).
55. Tony Liss, these proceedings.
56. C. Albajar, *et al.* (UA1 Collaboration), Z. Phys. **C 48** 1 (1990).
57. T. Akesson, *et al.* (UA2 Collaboration), Z. Phys. **C 46** 179 (1990).
58. F. Abe *et al.* (CDF Collaboration), Phys. Rev. Lett., **64** 147 (1990).
59. F. Paige and S. Protopopescu, BNL-38034 (1986); and in Proceedings of the 1986 Summer Study on the Physics of the Superconducting Supercollider, Donaldson, R. and Marx, J. ed, 320 (1986).
60. E. Eichten, Fermilab Preprint, Fermilab-Conf-90/29-T (1990).
61. J. Ohnemus, Florida State University Preprint FSU-HEP-910320 (1991).
62. John Ellis, presented at the International Lepton-Photon Symposium, Geneva, Switzerland, 25 July- 1 August 1991.
63. F.A. Berends *et al.*, Fermilab Preprint FERMILAB-Pub-90/213-T (1990).
64. R.K. Ellis, FERMILAB-Conf-89/168-T (1989).
65. G. Unal and L. Fayard, in " Proceedings of ECFA LHC Workshop", Aachen, FDR, CERN 90-10, ECFA 90-133, Ed. G. Jarlskog and D. Rein, 360 (1990).
66. S. Kuhlmann (CDF Collaboration), presented at the Second International Symposium on Particles, Strings and Cosmology, Northeastern University, Boston, Massachusetts, USA, March 25-30 (1991).